International Journal of Dynamics and Control (2023) 12:2689–2703
https://doi.org/10.1007/s40435-023-01370-8

Stability analysis of a discrete chaotic map in superior orbit

Renu[1] · **Ashish**[2] · **Renu Chugh**[3]

Received: 3 October 2023 / Revised: 10 December 2023 / Accepted: 11 December 2023 / Published online: 9 February 2024

Abstract
Discrete chaotic maps have found a pivotal place in the study of nonlinear dynamics and chaos theory, due to their significant applications in several disciplines including discrete traffic control, secure communications, cryptography, weather forecasting and the population biology of species. The stability analysis of discrete systems via different iterative orbits also plays a prominent role in studying the dynamical behavior of nonlinear systems. In this article, the stability performance of a discrete map is analyzed using two-step superior (Mann) iterative orbit through various dynamical aspects like fixed points, time-series analysis, period-doubling bifurcations and Lyapunov exponent. It is evident to notice that in the superior orbit, due to the freedom of an additional control parameter η, the discrete map admits an improved stability performance up to higher ranges of the growth-rate parameter ρ. Numerical simulations along with analytical analysis are used to examine the enhanced stability performance in the proposed discrete system. Further, the comparative bifurcation and Lyapunov diagrams report the superior stable behavior in the proposed system for decreasing values of parameter η and in contrast to the existing discrete systems. Thus, the superior stability performance of the discrete system may be used for improved control-based applications like traffic control and population control in the future.

Keywords Discrete map · Superior orbit · Stability · Chaos · Period-doubling · Lyapunov exponent (LE)

Mathematics Subject Classification 34H10 · 37B25 · 37G15 · 37H15 · 37M10 · 37N35

1 Introduction

A dynamical system is a system that evolves its state in a given time span according to some fixed rule/formula. This evolution can take place either smoothly over time or in discrete time steps. In this way, a dynamical system may be classified as a continuous or discrete dynamical system. Dynamical systems are mainly described by differential equations or discrete difference maps based on the time varying parameters. Further, a chaotic discrete system is one where this evolution displays an extreme sensitivity to the initial conditions in such a way that it is quite impossible to anticipate the long-run performance of the nonlinear system. Poincare [35] initially studied the chaotic dynamics of nonlinear systems followed by the seminal research work of Lorenz [25] and May [29] based on the computing of differential and discrete difference equations. One of the celebrated discrete chaotic map is the standard logistic system, also known as Verhulst model of population growth, given by the difference equation $x_{n+1} = \rho x_n(1-x_n)$, where $\rho > 0$ is the growth-rate parameter of population and $x_n \in [0, 1]$ denotes the population after n generations. In this model, for extremely low growth rate, the population will die out with going to extinction and higher growth rates may settle to a stable state or vibrates among population booms and busts series. Detailed discussions on discrete chaotic maps can be found in numerous other references, for example, Alligood et al. [1], Ausloos and Dirickx [8], Devaney [13, 14], Diamond [15], Mira [32], Elagdi [16], Elhadj and Sprott [17], Holm-

✉ Renu
renubadsiwal9@gmail.com

Ashish
akrmsc@gmail.com

Renu Chugh
chugh.rl@gmail.com

[1] Department of Mathematics, Maharshi Dayanand University, Rohtak, Haryana 124001, India

[2] Department of Mathematics, Government College Satnali, Mahendergarh, Haryana 123024, India

[3] Department of Mathematics, Gurugram University, Gurugram, Haryana 122003, India

gren [21], Melo and Van Strien [31], Martelli [28], Robinson [41], Mira et al. [33], Strogatz [47], and Wiggins [49].

Due to their richness in knowledge and implication, in twenty-first century, various discrete chaotic maps have found prominent applications in several engineering and scientific disciplines like transportation problems, image processing, neural network, data transmission, and cryptography. In 1990, Chowdhury and Debnath [10] studied about chaos and periodicity in a modulated logistic map. Andrecut [2] in 1997 explored that chaotic random number generation may be a powerful tool for computer simulation processes. Baptista [9] examined the text messages encryption scheme using chaotic maps in 1998. The traffic flow data were examined by Shang et al. [44] in 2005 by using time-series analysis, and they reported that the traffic flow on road exhibits chaotic dynamics. Lo and Cho [24] also proposed a discrete traffic flow model to tackle chaotic traffic on the road. In 2008, a novel cryptosystem using discrete chaotic maps was proposed by de Oliveira and Sobottka [18]. A chaotic noise analog generator design based on logistic map was developed by Medina et al. [30] in 2009. Further, Singh and Sinha [46] developed a secure communication system and established chaotic signals via discrete logistic map in 2010. In 2013, Radwan et al. [36] proposed some generalized discrete chaotic maps with improved applications in secure communication of data. Sayed et al. [43] also introduced designs of generalized logistic map with different signs in 2015. Effah-Poku et al. [19] examined the chaotic dynamics of nonlinear systems in 2018. For more applications of discrete chaotic maps, one can refer to Sharkovsky et al. [45], Crownover [12], Peitgen et al. [34], Harikirishnan and Nandkumaran [20], Malek and Gobal [26], Kocarev and Jakimoski [22], Rocha and Taha [42], and Wackerbauer et al. [48].

To enhance the stability performance and predictability of the discrete logistic map up to larger extent of the growth-rate parameter ρ which is useful for several applications, distinct iterative orbits and feedback methods were applied so far (see [3–5, 11, 37, 38] and other references therein). Moreover, different researchers have also studied various generalizations of discrete chaotic maps (see [6, 7, 10, 20, 36, 39, 40, 43]). Mann [27] in 1953 proposed a novel two-step feedback algorithm also termed as Mann (superior) iterative orbit and reported its improved convergence as compared to the one-step Picard iterative orbit. Thus, the Mann (superior) iterates aid in exploring the dynamical performance of discrete chaotic maps in a better way. In 2018–19, Ashish et al. [3–5] examined the dynamics of standard discrete logistic system using two-step superior iterative orbit and also proposed an enhanced model of traffic control. Further, in 2022 Kumar et al. [23] examined the dynamical performance of another one-dimensional standard chaotic map using various techniques. They reported that the chaos and stability performance of their proposed map are better as compared to the standard logistic map. Following these works and wider applications of discrete chaotic maps, in this article, we examine the discrete chaotic map proposed by Kumar et al. [23] in superior orbit that displays improved stability performance than the existing chaotic systems. Thus, the superiority in stability range makes the discrete system in superior orbit a better fit for different control-based applications such as population control and traffic control on the road.

The article is arranged into five distinct sections. An introduction along with brief literature survey is provided in Sect. 1, while Sect. 2 presents the basic terminology used in the study. Section 3 reports the formulation and analysis of the discrete system in superior (Mann) orbit, where the superior stability performance of the system is disclosed through fixed state evolution, time-series study, period-doubling bifurcations and Lyapunov exponent analysis. Moreover, a comparative analysis of the superior stability performance of the discrete system through bifurcation and Lyapunov plots along with possible applications is presented in Sect. 4. At last, Sect. 5 concludes the whole article.

2 Basic definitions

This section deals with the key terminology and facts which are used in the analysis of discrete maps.

Definition 2.1 *(Superior orbit)* [27]: Suppose $f : X \to X$ denotes a discrete map defined on a non-empty set X. Then, the sequence of iterations $\{x_n\}$, for an initial choice $x_0 \in X$, defined as

$$x_{n+1} = (1 - \eta_n)x_n + \eta_n f(x_n), \tag{1}$$

where $\eta_n \in [0, 1]$, $n = 0, 1, 2, 3, \ldots$, is called Mann (superior) iteration orbit, and the entire system is termed as a two-step superior iterative system as it needs two numbers, say, η and x_0, as input to give a new output number. For $\eta_n = 1$, the system (1) changes to the traditional system $x_{n+1} = f(x_n)$.

Definition 2.2 *(Fixed and periodic point)* [13]: For a discrete map $f : X \to X$ defined on a non-empty set X, a point $x \in X$ is said to be fixed if $f(x) = x$ and a periodic point of period-m for $f^m(x) = x$, where m denotes the smallest positive integer and the iteration sequence $\{x_1, x_2, \ldots, x_m\}$ is known as an orbit of period-m.

Definition 2.3 *(Attracting and repelling fixed point)* [14]: For a discrete map $f : X \to X$, where X is a non-empty set, a fixed point $x \in X$ is called attracting if $|f'(x)| < 1$ and repelling for $|f'(x)| > 1$. Also, that fixed point is known as neutral or weakly attracting for $|f'(x)| = 1$.

Definition 2.4 *(Chain rule of differentiation for a cycle)* [14]: For a discrete map $f : X \to X$, where X is a non-empty set,

if $\{x_1, x_2, \ldots, x_n\}$ denotes an iteration sequence lying on a period-n cycle. Then, the derivative of n^{th} iteration of the system f is given as,

$$(f^n)'(x_1) = f'(x_1) \times f'(x_2) \times \cdots \times f'(x_{n-1}) \times f'(x_n), \tag{2}$$

i.e., the derivative of f^n at point x_1 is the multiplication of the derivatives of f on each point of the cycle.

Definition 2.5 *(Lyapunov exponent)* [1]: For a discrete map $f : \mathbb{R} \to \mathbb{R}$ defined on the set of reals $\mathbb{R}$, the Lyapunov exponent (γ), for an iterative orbit $\{x_n\}$, is defined as

$$\gamma(x_1) = \lim_{n\to\infty} \frac{1}{n} \sum_{k=1}^{n} \log|f'(x_k)|, \tag{3}$$

such that the limit exists finitely. The system exhibits fixed stable and periodic behavior for LE $(\gamma) < 0$ and chaos or unstable state for $\gamma > 0$. Also, for $\gamma = 0$, the system depicts a neutral state. Hence, the Lyapunov exponent value helps in examining the stable and unstable behaviors of the system.

3 Formulation and analysis of the superior discrete chaotic system $T_{\eta,\rho}(x)$

Let us consider a discrete chaotic map [23] defined as below:

$$k_\rho(x) = \frac{\rho x(1-x)}{1+x}, \text{ where } \rho > 0, \text{ and } x \in [0, 1]. \tag{4}$$

Further, the difference equation form of the above map can be given as:

$$x_{n+1} = k_\rho(x_n) = \frac{\rho x_n(1-x_n)}{1+x_n}, \text{ where } \rho > 0,\ x_n \in [0, 1] \text{ and } n = 0, 1, 2, \ldots \tag{5}$$

Then, for an initial choice $x_0 \in [0, 1]$, the next iterate x_1 of the discrete map (5) via the superior two-step iterative system (Definition 2.1) can be derived as:

$$x_1 = (1-\eta_0)x_0 + \eta_0 k_\rho(x_0), \text{ where } k_\rho(x_0) = \frac{\rho x_0(1-x_0)}{1+x_0}.$$

Through induction, the discrete map (5) form in superior (Mann) orbit is given by:

$$x_{n+1} = (1-\eta_n)x_n + \eta_n k_\rho(x_n), \text{ where } \eta_n \in [0, 1],\ x_n \in [0, 1] \text{ and } n = 0, 1, 2, \ldots \tag{6}$$

Now, it is evident that for $\eta_n = 0$, the system (6) admits an obvious state $x_{n+1} = x_n$ and for $\eta_n = 1$, it reduces to the standard discrete map (5). So, for an authenticity of the article, we consider $\eta_n \in (0, 1)$. Thus, by assuming $\eta_n = \eta$, $x_n = x$ and putting (5) in (6), the proposed variation of the discrete map (5) in the superior (Mann) orbit changes to the following form:

$$T_{\eta,\rho}(x) = (1-\eta)x + \eta\left(\frac{\rho x(1-x)}{1+x}\right), \tag{7}$$

where $x \in [0, 1]$ and $T_{\eta,\rho}(x)$ denotes the superior discrete system with $\eta \in (0, 1)$ and $\rho > 0$ as its two control parameters. In this article, we consider the parameter values $\eta = 0.9, 0.55$ and 0.2 to examine the stability performance of the system $T_{\eta,\rho}(x)$.

3.1 Fixed point analysis for the superior system $T_{\eta,\rho}(x)$ at $\eta = 0.9, 0.55$ and 0.2

For the discrete system $T_{\eta,\rho}(x)$ given in (7), a sequence of iterations defined as $\{x_0,\ T_{\eta,\rho}(x_0) = x_1,\ T^2_{\eta,\rho}(x_0) = x_2,\ T^3_{\eta,\rho}(x_0) = x_3,\ \ldots,\ T^n_{\eta,\rho}(x_0) = x_n, \ldots\}$ is called an iterative orbit with an initial input or seed $x_0 \in [0, 1]$ and $T^n_{\eta,\rho}(x_0)$ denotes the n^{th} iterate of $T_{\eta,\rho}(x)$ at point x_0.

Further, from Definition 2.2 using relation (7), the fixed point iterative orbit for the system $T_{\eta,\rho}(x)$ may be written as the iterative sequence $\{x_0,\ T_{\eta,\rho}(x_0) = x_0,\ T^2_{\eta,\rho}(x_0) = x_0,\ T^3_{\eta,\rho}(x_0) = x_0,\ \ldots,\ T^n_{\eta,\rho}(x_0) = x_0, \ldots\}$ or $\{x_0, x_0, \ldots, x_0, \ldots\}$, where $x_0 \in [0, 1]$ is the initial choice. Now, we explore the general fixed point properties for the superior discrete system $T_{\eta,\rho}(x)$.

As we have $T_{\eta,\rho}(x) = (1-\eta)x + \eta\left(k_\rho(x)\right)$, where $k_\rho(x) = \frac{\rho x(1-x)}{1+x}$, then, by using Definition 2.2 of fixed point, it may be written as:

$$\begin{aligned}
& T_{\eta,\rho}(x) = x, \\
\text{that is,}\quad & (1-\eta)x + \eta\left(\frac{\rho x(1-x)}{1+x}\right) = x, \\
& (1-\eta)(1+x)x + \eta\rho x(1-x) = x(1+x), \\
& x(\eta\rho - \eta - \eta\rho x - \eta x) = 0, \\
\text{either}\quad & x = 0 \text{ or } \eta(\rho - 1 - \rho x - x) = 0, \\
\therefore\quad & x = 0 \text{ and } \rho - 1 - \rho x - x = 0 \quad (\because \eta > 0), \\
\text{that is,}\quad & x = 0 \text{ and } x = \frac{\rho - 1}{\rho + 1} \text{ for } \rho > 0.
\end{aligned}$$

Thus, $p_1 = 0$ and $p_2 = \frac{\rho-1}{\rho+1}$ for $\rho > 0$ are the two fixed points for the discrete system $T_{\eta,\rho}(x)$ for each $\eta \in (0, 1)$. Also, it is evident to notice that the non-trivial fixed point $p_2 = \frac{\rho-1}{\rho+1}$ lies in [0,1] for all $\rho > 1$. Thus, the discrete system $T_{\eta,\rho}(x)$ reveals only the trivial fixed point $p_1 = 0$ for $0 < \rho \leq 1$ and the two fixed points $p_1 = 0$ and $p_2 = \frac{\rho-1}{\rho+1}$ for $\rho > 1$ as depicted in Fig. 1a, b, respectively.

Attracting and repelling fixed points versus parameters η and ρ in the superior system $T_{\eta,\rho}(x)$

Here, for distinct values of the control parameter η, we examine the respective ranges of growth-rate parameter ρ, for which fixed points p_1 and p_2 of the system $T_{\eta,\rho}(x)$ are in attracting and repelling states. So, by using Definition 2.3 of attracting and repelling fixed points for the system $T_{\eta,\rho}(x)$, we have "A fixed point x for the system $T_{\eta,\rho}$ is called attracting if $|T'_{\eta,\rho}(x)| < 1$ and repelling for $|T'_{\eta,\rho}(x)| > 1$. Also, the fixed point is known as neutral or weakly attracting for $|T'_{\eta,\rho}(x)| = 1$". As, we have

$$T_{\eta,\rho}(x) = (1-\eta)x + \eta\left(\frac{\rho x(1-x)}{1+x}\right)$$

$$\text{Then,}\quad T'_{\eta,\rho}(x) = (1-\eta) + \eta\rho\left(\frac{1-2x-x^2}{(1+x)^2}\right). \tag{8}$$

Now, we consider three distinct values of the control parameter η:

(a) For $\eta = 0.9$

As $p_1 = 0$ and $p_2 = \frac{\rho-1}{\rho+1}$ are two fixed points of the system $T_{\eta,\rho}(x)$ for each $\eta \in (0,1)$, for fixed point $p_1 = 0$, using (8), we get $|T'_{0.9,\rho}(0)| = |1-\eta+\eta\rho| = |1-(0.9)+(0.9)\times\rho| < 1$ for $0 < \rho < 1$. Also, $|T'_{0.9,\rho}(0)| = 1$ for $\rho = 1$ and $|T'_{0.9,\rho}| > 1$ for $\rho > 1$. Thus, the fixed point $p_1 = 0$ is attracting for $0 < \rho < 1$, neutral (weakly attracting) at $\rho = 1$ and repelling for $\rho > 1$ for the system $T_{0.9,\rho}(x)$.

Likewise, for other fixed point $p_2 = \frac{\rho-1}{\rho+1}$, by using relation (8), we have

$$\left|T'_{\eta,\rho}(p_2)\right| = \left|(1-\eta) + \eta\rho\left(\frac{1-2p_2-p_2^2}{(1+p_2)^2}\right)\right|$$

$$\text{that is,}\quad \left|T'_{0.9,\rho}\left(\frac{\rho-1}{\rho+1}\right)\right| = |(1-0.9)+(0.9)\times\rho \times\left(\frac{1-2\times\left(\frac{\rho-1}{\rho+1}\right)-\left(\frac{\rho-1}{\rho+1}\right)^2}{\left(1+\left(\frac{\rho-1}{\rho+1}\right)\right)^2}\right)\Bigg|. \tag{9}$$

By solving (9), we find that $|T'_{0.9,\rho}(p_2)| < 1$ for $1 < \rho < 4.66$. Further, $|T'_{0.9,\rho}(p_2)| = 1$ at $\rho = 4.66$ and $|T'_{0.9,\rho}(p_2)| > 1$ for $\rho > 4.66$. Hence, by Definition 2.3, the fixed point p_2 of the system $T_{\eta,\rho}(x)$ is attracting for $1 < \rho < 4.66$, neutral for $\rho = 4.66$ and repelling for $\rho > 4.66$, at $\eta = 0.9$.

(b) For $\eta = 0.55$

Likewise, as discussed in case (a), for the trivial fixed point 0, using (8), we have $|T'_{0.55,\rho}(0)| = |1-(0.55)+(0.55)\times\rho| < 1$ for $0 < \rho < 1$. So, the fixed point $p_1 = 0$ of $T_{0.55,\rho}(x)$ is attracting for $0 < \rho < 1$, neutral for $\rho = 1$ and repelling for $\rho > 1$. Further, for the fixed point $p_2 = \frac{\rho-1}{\rho+1}$, we get

$$\left|T'_{0.55,\rho}\left(\frac{\rho-1}{\rho+1}\right)\right| = |(1-0.55)+(0.55)\times\rho \times\left(\frac{1-2\times\left(\frac{\rho-1}{\rho+1}\right)-\left(\frac{\rho-1}{\rho+1}\right)^2}{\left(1+\left(\frac{\rho-1}{\rho+1}\right)\right)^2}\right)\Bigg|. \tag{10}$$

Now, simplifying (10), we get $|T'_{0.55,\rho}(p_2)| < 1$ for $1 < \rho < 7.41$. Thus, in turn, the fixed point p_2 of $T_{0.55,\rho}(x)$ is attracting for $1 < \rho < 7.41$, neutral for $\rho = 7.41$ and repelling for $\rho > 7.41$.

(c) For $\eta = 0.2$

Using (8), for $\eta = 0.2$ and fixed point $p_1 = 0$, we find $|T'_{0.2,\rho}| = |1-(0.2)+(0.2)\times\rho| < 1$ for $0 < \rho < 1$. Hence, 0 is an attracting fixed point for $0 < \rho < 1$ and neutral and repelling fixed point for $\rho = 1$ and $\rho > 1$, respectively. Similarly, for $p_2 = \frac{\rho-1}{\rho+1}$ in this case, we obtain

$$\left|T'_{0.2,\rho}\left(\frac{\rho-1}{\rho+1}\right)\right| = |(1-0.2)+(0.2)\times\rho \times\left(\frac{1-2\times\left(\frac{\rho-1}{\rho+1}\right)-\left(\frac{\rho-1}{\rho+1}\right)^2}{\left(1+\left(\frac{\rho-1}{\rho+1}\right)\right)^2}\right)\Bigg|. \tag{11}$$

By solving (11), we get $|T'_{0.2,\rho}(p_2)| < 1$ for $1 < \rho < 20.05$ and hence the fixed point p_2 of $T_{0.2,\rho}(x)$ displays attracting, neutral and repelling states for $1 < \rho < 20.05$, $\rho = 20.05$ and $\rho > 20.05$, respectively.

It is evident from the above analysis that the obvious fixed point $p_1 = 0$ is in attracting (stable) state for $0 < \rho \leq 1$ for each $\eta \in (0,1)$, whereas the other fixed point $p_2 = \frac{\rho-1}{\rho+1}$ is attracting (stable) in the respective ranges of parameter ρ for distinct values of parameter $\eta \in (0,1)$, that is, for $1 < \rho \leq 4.66$, $1 < \rho \leq 7.41$ and $1 < \rho \leq 20.05$ at $\eta = 0.9, 0.55$ and 0.2, respectively. The cobweb plots in Fig. 2a–d display the attracting behavior of fixed points 0 and $\frac{\rho-1}{\rho+1}$ of $T_{\eta,\rho}(x)$ for different values of parameters η and ρ.

Remark 3.1 The growth-rate parameter ranges for the attracting behavior of the non-trivial fixed point p_2 at $\eta = 0.9, 0.55, 0.2$ are $1 < \rho \leq 4.66$, $1 < \rho \leq 7.41$ and $1 < \rho \leq 20.05$, respectively. Thus, the respective attracting (stable) range of the fixed point p_2 increases when the parameter value η decreases.

3.2 Time-series representation in the superior system $T_{\eta,\rho}(x)$ for $\eta = 0.9, 0.55$ and 0.2

This section presents the time-series representation of the system $T_{\eta,\rho}(x)$ by changing the parameters η and ρ in their

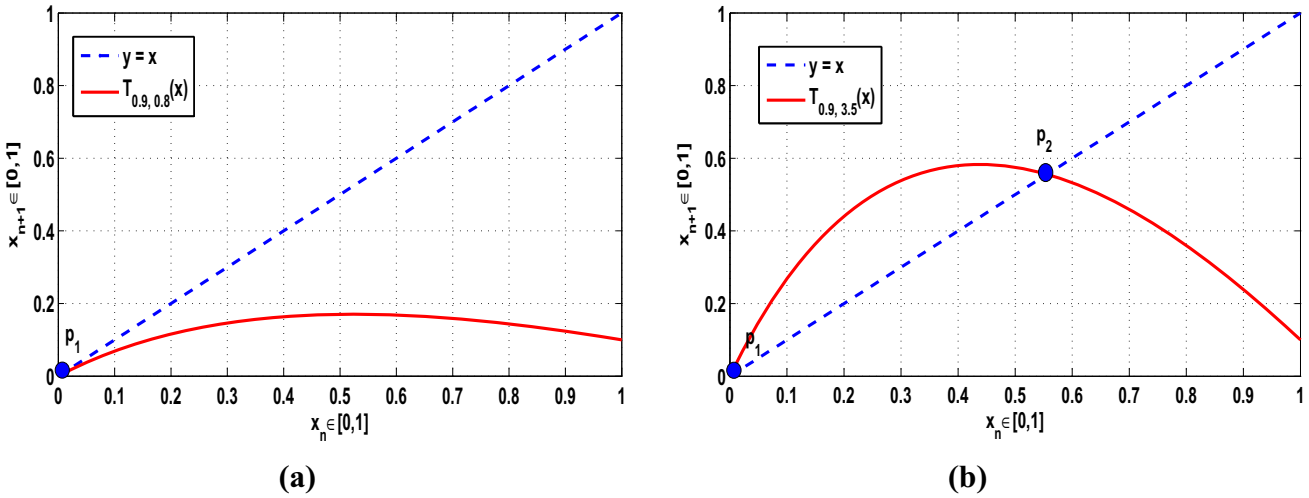

Fig. 1 For the system $T_{\eta,\rho}(x)$, graphical representation of **a** only the trivial fixed point p_1 at $\eta = 0.9$ and $\rho = 0.8$, **b** two fixed points p_1 and p_2 at $\eta = 0.9$ and $\rho = 3.5$

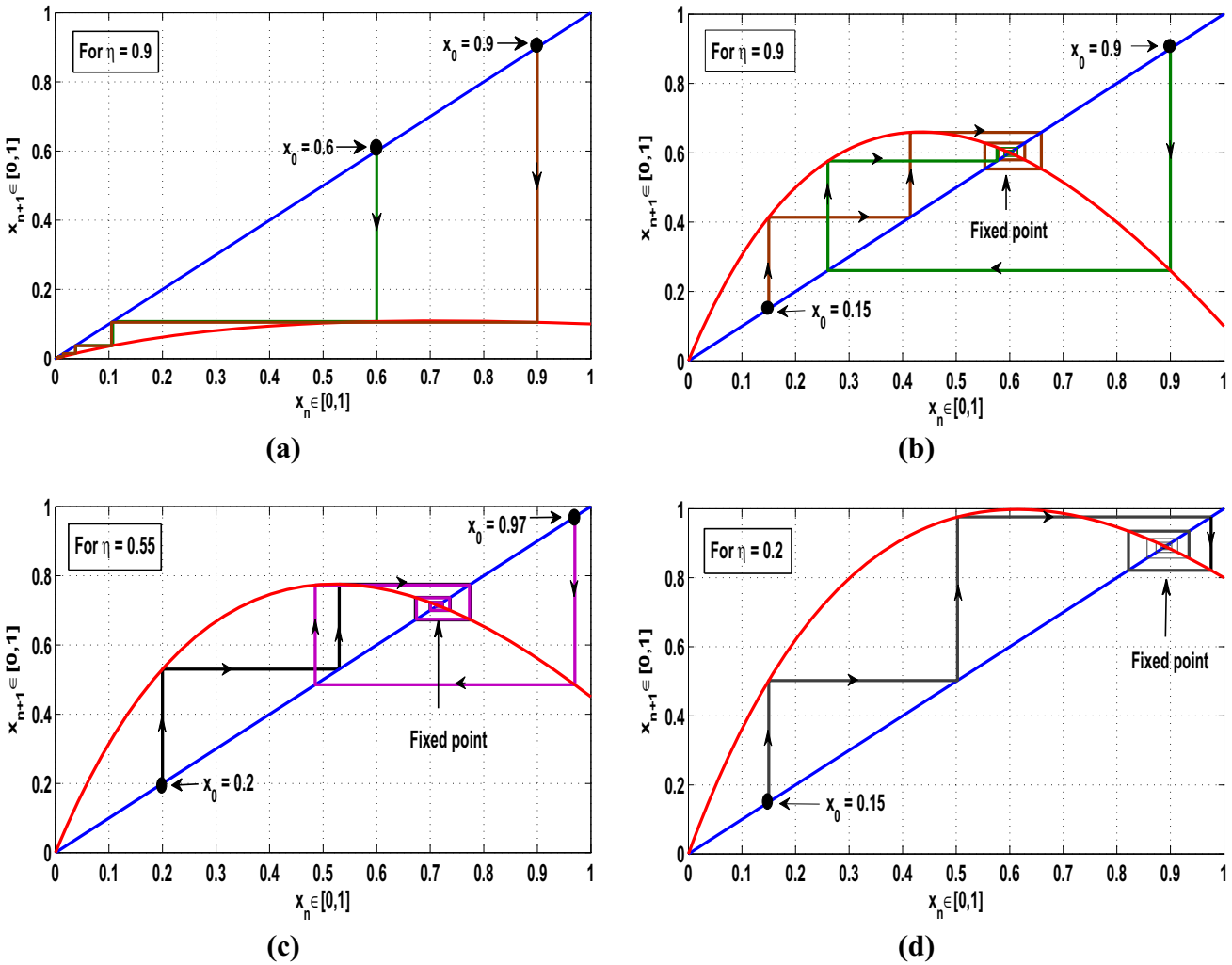

Fig. 2 For $T_{\eta,\rho}(x)$, **a** attracting nature of fixed point 0 at $\eta = 0.9$, $\rho = 0.8$ and attracting behavior of fixed point $\frac{\rho-1}{\rho+1}$ for **b** $\eta = 0.9$, $\rho = 4$, **c** $\eta = 0.55$, $\rho = 6$, **d** $\eta = 0.2$, $\rho = 17.25$

specific extent. Figures 3 and 4 depict the time-series plots of $T_{\eta,\rho}(x)$ at $\eta = 0.9$, 055 and 0.2.

(a) For $\eta = 0.9$

The superior system $T_{\eta,\rho}(x)$ admits fixed state, periodic behavior and chaos for $\eta = 0.9$ and $0 < \rho \leq 6.2$ as shown in Fig. 3a–d. Also, Fig. 3a depicts that the iterative orbit of the system $T_{0.9,\rho}(x)$ tends to the trivial fixed point $p_1 = 0$ for $0 < \rho \leq 1$ and to the non-trivial fixed point $p_2 = \frac{\rho-1}{\rho+1}$ for $1 < \rho \leq 4.66$. For $4.66 < \rho \leq 5.54$, the system oscillates between period-2 stable solutions and period-4 vibrations exist in the system for $5.54 < \rho \leq 5.71$ as depicted in Fig. 3b, c, respectively. These 2^n periodic oscillations continue in the system up to $\rho = 5.76$. As $\rho_\infty \approx 5.76$, the system $T_{0.9,\rho}(x)$ enters into an irregular state and exhibits chaos for $5.76 < \rho \leq 6.2$ as shown in Fig. 3d. Moreover, for $\rho > 6.2$, the system $T_{0.9,\rho}$ is undefined, as there exists at least one such x_n that does not lie in [0,1].

(b) For $\eta = 0.55$

The system displays fixed state and periodicity for $\eta = 0.55$ and $0 < \rho \leq 8.49$ as shown in Fig. 4a–c. Further, Fig. 4a depicts the convergence in the system to the obvious fixed point 0 for $0 < \rho \leq 1$ and to the non-trivial fixed point $\frac{\rho-1}{\rho+1}$ for $1 < \rho \leq 7.41$. Period-2 stable vibrations exist in the system for $7.41 < \rho \leq 8.49$ as shown in Fig. 4b. Also, for $\rho > 8.49$, the system is undefined, as there is at least one such x_n that does not lie in the interval [0, 1] (see Fig. 4c).

(c) For $\eta = 0.2$

Figure 4d–f represents the time-series plots of the system for $\eta = 0.2$ and $0 < \rho \leq 20.25$. In particular, Fig. 4d shows the fixed point convergence for the system to the obvious fixed point 0 for $0 < \rho \leq 1$ and to the non-trivial fixed point p_2 for $1 < \rho \leq 20.05$, whereas the period-2 stable oscillations in the system for $20.05 < \rho \leq 20.25$ are depicted in Fig. 4e. For $\eta > 20.25$, the system $T_{0.2,\rho}(x)$ does not exist as x_n does not lie entirely in [0, 1] there as depicted in Fig. 4f.

3.3 Periodic evolution of the superior system $T_{\eta,\rho}(x)$ for $\eta = 0.9$, 0.55 and 0.2

Periodic evolution, another leading aspect in nonlinear systems, is generally used to examine the dynamical performance of discrete systems, by reporting the period-doubling character of different iterative orbits of the system. This section put forward the period-doubling bifurcations versus the parameters η and ρ for the system $T_{\eta,\rho}(x)$. So, for an initial choice $x_0 \in [0, 1]$, with step size 0.001 and $\eta = 0.9, 0.55, 0.2$, the period-doubling diagrams are presented in Figs. 5 and 6, respectively.

(a) For $\eta = 0.9$

Figure 5a displays the complete bifurcation plot of the system $T_{0.9,\rho}(x)$. Further, it is evident from Fig. 5b that as $\rho \approx 4.66$, the non-trivial fixed point $p_2 = \frac{\rho-1}{\rho+1}$ turns into an unstable state and initial bifurcation in the system comes into picture, where the system vibrates between period-2 stable branches B_1 and B_2 for $4.66 < \rho \leq 5.54$. In similar fashion, for $\rho > 5.54$, the next period-doubling appears in the system; that means, for $5.54 < \rho \leq 5.71$ the stable branches B_1 and B_2 of period-2 become unstable and the system $T_{0.9,\rho}(x)$ starts to oscillate among period-4 stable branches B_{11}, B_{12}, B_{21} and B_{22}. Also, other higher 2^n-order bifurcations in the system are reported for $5.71 < \rho \leq 5.76$. As $\rho_\infty \approx 5.76$, a transition from period-doubling to the chaotic evolution is noticed in the system. The full-fledged chaos performance of the system in the magnified form for the parameter range $5.76 < \rho \leq 6.2$ can be visualized in Fig. 5c. Moreover, for $\rho > 6.2$, the system $T_{0.9,\rho}(x)$ cannot be defined, as it exceeds 1 there; that means, the value of ρ_{max} for the system $T_{0.9,\rho}(x)$ is 6.2 (see Fig. 5a).

(b) For $\eta = 0.55$

Figure 6a–b depicts the bifurcations plots of the system $T_{0.55,\rho}(x)$. Further, Fig. 6a clarifies that the non-trivial fixed point $p_2 = \frac{\rho-1}{\rho+1}$ becomes unstable for $\rho > 7.41$ and the system $T_{0.55,\rho}(x)$ alternates between period-2 stable branches B_1 and B_2 for $7.41 < \rho \leq 8.49$. Also, when the growth-rate parameter ρ exceeds 8.49, i.e., for $\rho > 8.49$, the system $T_{0.55,\rho}(x)$ is not defined, since x_n does not lie in [0, 1] there as shown in Fig. 6b. Thus, the value of p_{max} for $T_{0.55,\rho}(x)$ is 8.49 (see Fig. 6a, b).

(c) For $\eta = 0.2$

Figure 6c shows that the system $T_{0.2,\rho}(x)$ admits convergence to the obvious fixed point 0 for $0 < \rho \leq 1$ and to the non-trivial fixed point solution $\frac{\rho-1}{\rho+1}$ for $1 < \rho \leq 20.05$ along with stable period-2 oscillations in the parameter range $20.05 < \rho \leq 20.25$. In addition, for $\rho > 20.25$, the iterative orbit $x_n \notin [0, 1]$, and thus, the discrete system $T_{0.2,\rho}(x)$ does not exist there, as depicted in Fig. 6d. In this way, the value of parameter ρ_{max} for the system $T_{0.2,\rho}(x)$ is 20.25 (see Fig. 6c, d).

Remark 3.2 For $\eta = 0.9$, 0.55 and 0.2, the values of parameter ρ_{max} are 6.2, 8.49 and 20.25, respectively (see Figs. 5a and 6b, d). Hence, the value of growth-rate parameter ρ_{max} increases when the value of control parameter η decreases.

Remark 3.3 The growth-rate parameter (ρ) extents corresponding to the stable behavior of the system $T_{\eta,\rho}(x)$ for $\eta = 0.9$, 0.55 and 0.2 are reported as $0 < \rho \leq 5.76$ (Fig. 5a, b), $0 < \rho \leq 8.49$ (Fig. 6a, b) and $0 < \rho \leq 20.25$ (Fig. 6c, d), respectively. Thus, the respective range for stability performance in the system increases when we decrease the value of control parameter η.

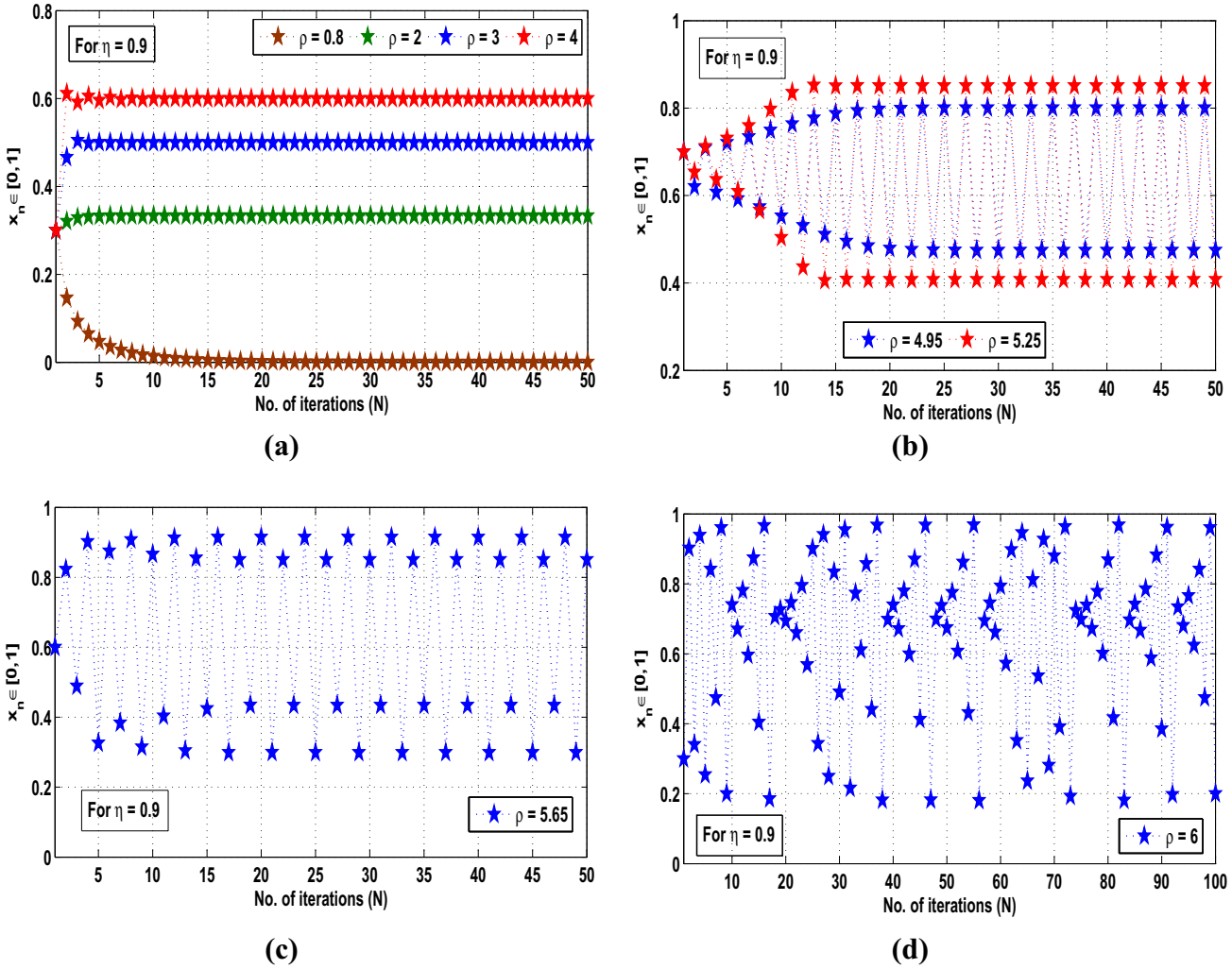

Fig. 3 For the superior system $T_{\eta,\rho}(x)$, **a** fixed stable solutions at $\eta = 0.9; \rho = 0.8,\ 2,\ 3$ and 4, **b** period-2 stable vibrations at $\eta = 0.9$; $\rho = 4.95$ and 5.25, **c** period-4 stable vibration at $\eta = 0.9$ and $\rho = 5.65$, **d** unstable vibration at $\eta = 0.9$ and $\rho = 6$

3.4 Maximal Lyapunov exponent in the superior system $T_{\eta,\rho}(x)$ for $\eta = 0.9$, 0.55 and 0.2

This section presents the maximal Lyapunov exponent (MLE), a tremendous tool to characterize chaos, predictability of nonlinear systems and their sensitive dependence to initial conditions for distinct iteration orbits. So, for the system $T_{\eta,\rho}(x)$, the MLE is determined as follows:

Let x and $x+\xi$ for $0 < \xi < 1$ be the close initiators for two distinct orbits and D, defined as the exponential growth $\xi e^{n\gamma}$, denote the divergence between these orbits, where γ indicates the maximal Lyapunov exponent (MLE) of $T_{\eta,\rho}(x)$ and n signifies the number of iterations. So, we obtain

$$T^n_{\eta,\rho}(x+\xi) - T^n_{\eta,\rho}(x) = D = \xi e^{n\gamma},$$
$$\text{i.e.,}\quad \frac{T^n_{\eta,\rho}(x+\xi) - T^n_{\eta,\rho}(x)}{\xi} = e^{n\gamma}. \tag{12}$$

Taking limit $\xi \to 0$ at both sides, we have

$$\lim_{\xi\to 0} \frac{T^n_{\eta,\rho}(x+\xi) - T^n_{\eta,\rho}(x)}{\xi} = e^{n\gamma},$$
$$\text{i.e.,}\quad (T^n_{\eta,\rho})'(x) = e^{n\gamma}. \tag{13}$$

By taking logarithm at both sides of (13), we get

$$\gamma = \frac{1}{n}\log|(T^n_{\eta,\rho})'(x)|, \tag{14}$$

such that $\eta \in (0,1)$, $\rho > 0$ and $(T^n_{\eta,\rho})'(x)$ is the first derivative of $T^n_{\eta,\rho}(x)$. Further, for the iteration sequence $\{x_1, x_2 = T_{\eta,\rho}(x_1),\ x_3 = T_{\eta,\rho}(x_2),\ \ldots,\ x_{n+1} = T_{\eta,\rho}(x_n),\ \ldots\}$, the derivative for the n^{th} degree polynomial, i.e., $(T^n_{\eta,\rho})'(x_1)$, through Definition 2.4 of chain rule, may be defined as below:

$$(T^n_{\eta,\rho})'(x_1) = T'_{\eta,\rho}(x_n)\cdot T'_{\eta,\rho}(x_{n-1})\cdots T'_{\eta,\rho}(x_2)\cdot T'_{\eta,\rho}(x_1). \tag{15}$$

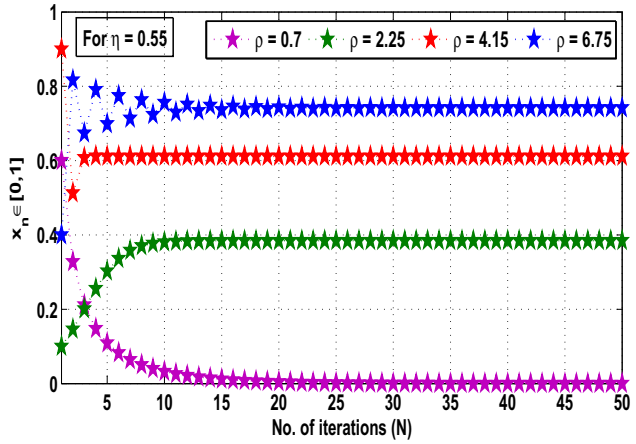

(a)

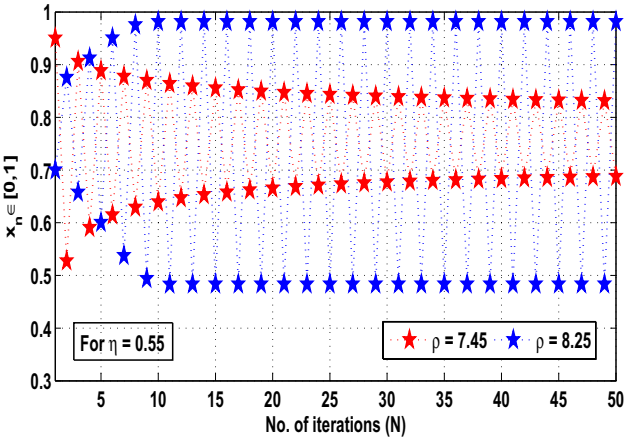

(b)

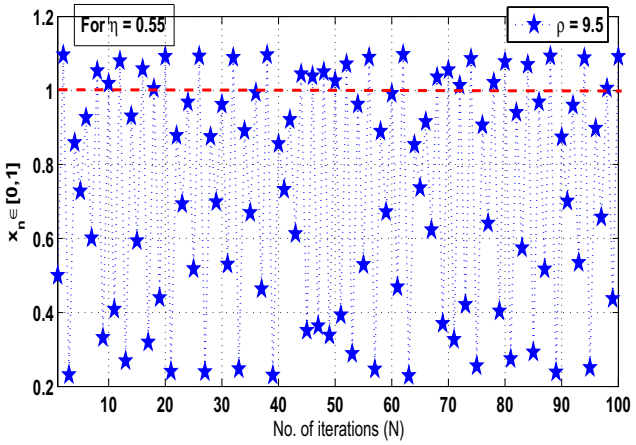

(c)

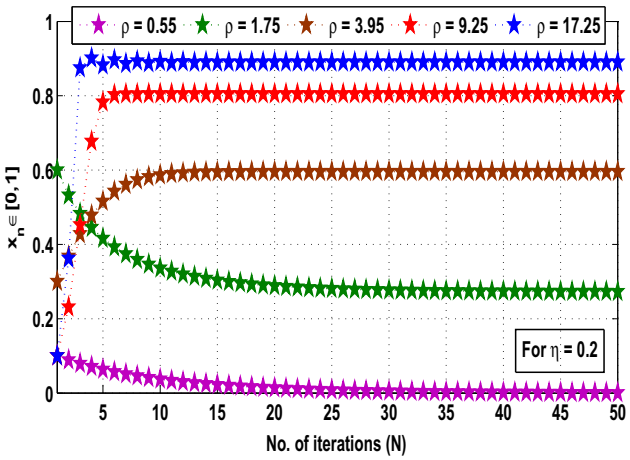

(d)

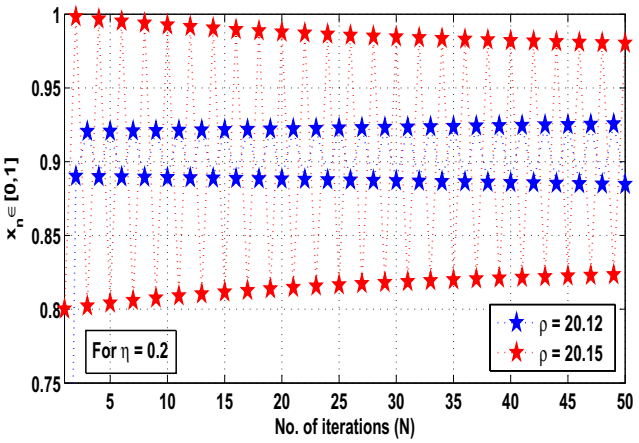

(e)

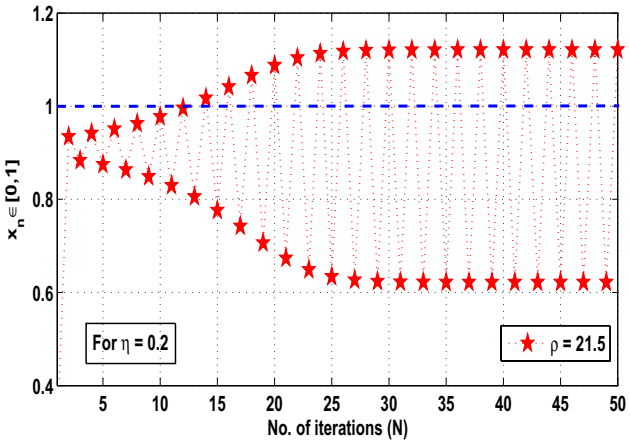

(f)

Fig. 4 For the system $T_{\eta,\rho}(x)$, **a** fixed stable solutions at $\eta = 0.55$; $\rho = 0.7, 2.25, 4.15, 6.75$, **b** period-2 stable vibrations at $\eta = 0.55$; $\rho = 7.45, 8.25$, **c** undefined vibration at $\eta = 0.55$, $\rho = 9.5$, **d** fixed stable solutions at $\eta = 0.2$; $\rho = 0.55, 1.75, 3.95, 9.25, 17.25$, **e** period-2 stable vibrations at $\eta = 0.2$; $\rho = 20.12, 20.15$, **f** undefined vibration at $\eta = 0.2$, $\rho = 21.5$

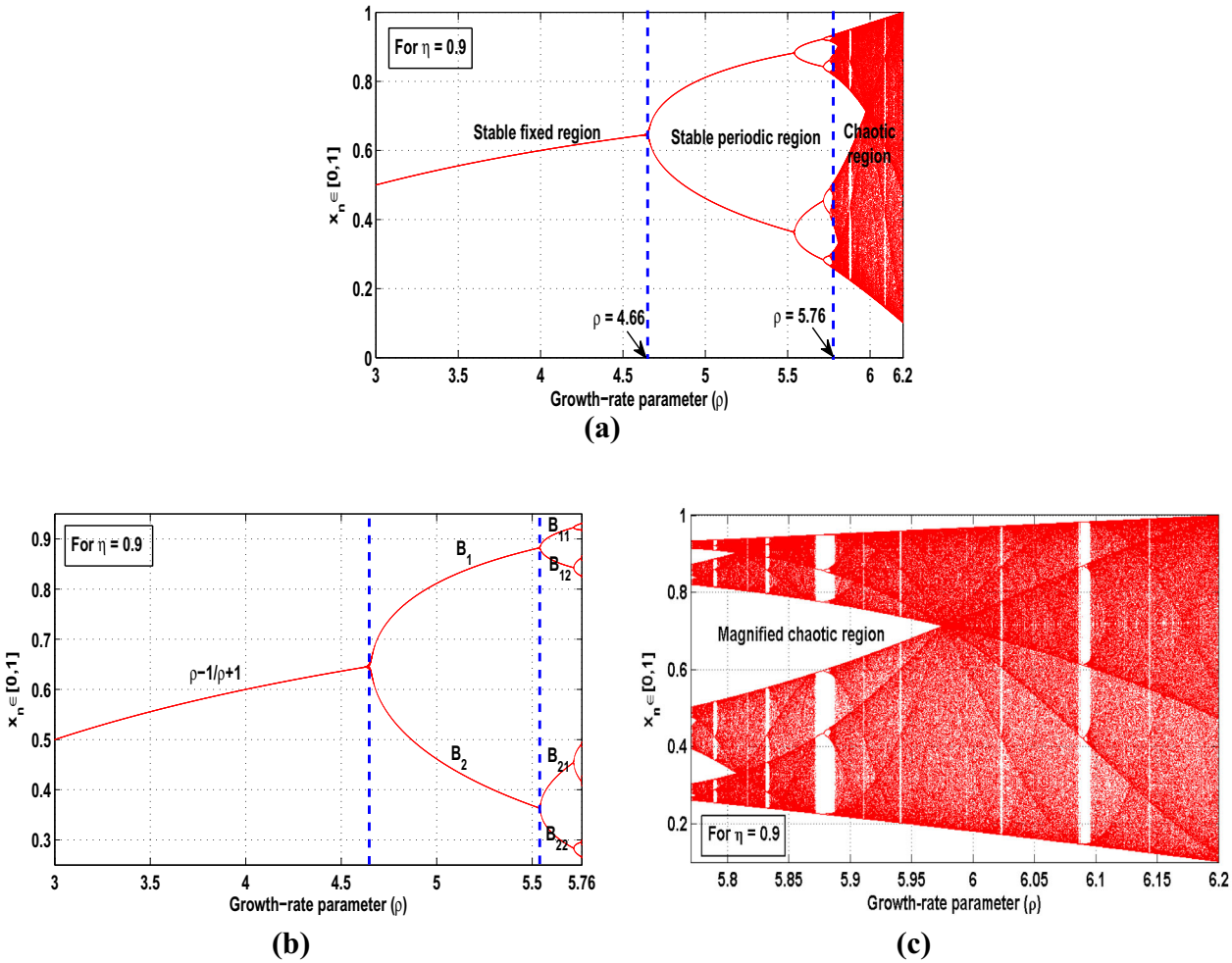

Fig. 5 For the system $T_{\eta,\rho}(x)$ at $\eta = 0.9$, $x_0 = 0.3$, $N = 500$, **a** bifurcation plot for $3 \le \rho \le 6.2$, **b** period-doubling plot for $3 \le \rho \le 5.76$, **c** magnified chaotic region for $5.77 \le \rho \le 6.2$

Thus, by (14) and (15), the maximal Lyapunov exponent (MLE) is given as:

$$\begin{aligned}\gamma &= \frac{1}{n}\log|T'_{\eta,\rho}(x_n)\cdot T'_{\eta,\rho}(x_{n-1})\ldots T'_{\eta,\rho}(x_2)\cdot T'_{\eta,\rho}(x_1)|,\\ &= \frac{1}{n}\Big[\log|T'_{\eta,\rho}(x_n)| + \log|T'_{\eta,\rho}(x_{n-1})| + \cdots\\ &\quad + \log|T'_{\eta,\rho}(x_2)| + \log|T'_{\eta,\rho}(x_1)|\Big],\\ &= \frac{1}{n}\sum_{k=1}^{n}\log|T'_{\eta,\rho}(x_k)|, \end{aligned} \tag{16}$$

where $\eta \in (0, 1)$ and $\rho > 0$. Thus, it is observed that the maximal Lyapunov exponent (γ) is equal to the average value of $\log|T'_{\eta,\rho}(x)|$ for the iteration sequence $\{x_n\}$ in the superior system $T_{\eta,\rho}(x)$. Moreover, the negative MLE (γ) signifies stable behavior in the system, whereas for the positive MLE(γ), the system exhibits chaotic or unstable behavior and admits more sensitivity on initial conditions.

For any fixed stable orbit of $T_{\eta,\rho}(x)$, the maximal Lyapunov exponent (γ) reduces to the form:

$$\gamma = \log|T'_{\eta,\rho}(x_1)|. \tag{17}$$

Moreover, for any periodic stable orbit of order m, MLE (γ) takes the following form:

$$\gamma = \frac{1}{m}\sum_{k=1}^{m}\log|T'_{\eta,\rho}(x_k)|. \tag{18}$$

As MLE estimation for aperiodic orbits, which are neither fixed nor periodic, using the entire length of orbits is practically impossible. So, MLE is evaluated by using only finite length of an iterative orbit.

Example 3.4 Let $T_{\eta,\rho}(x)$ be the superior discrete system and $k_\rho(x)$ be the original discrete map, where $\rho \in (0, 6.2]$ and $x \in [0, 1]$. Then, evaluate the maximum Lyapunov exponent (γ) for:

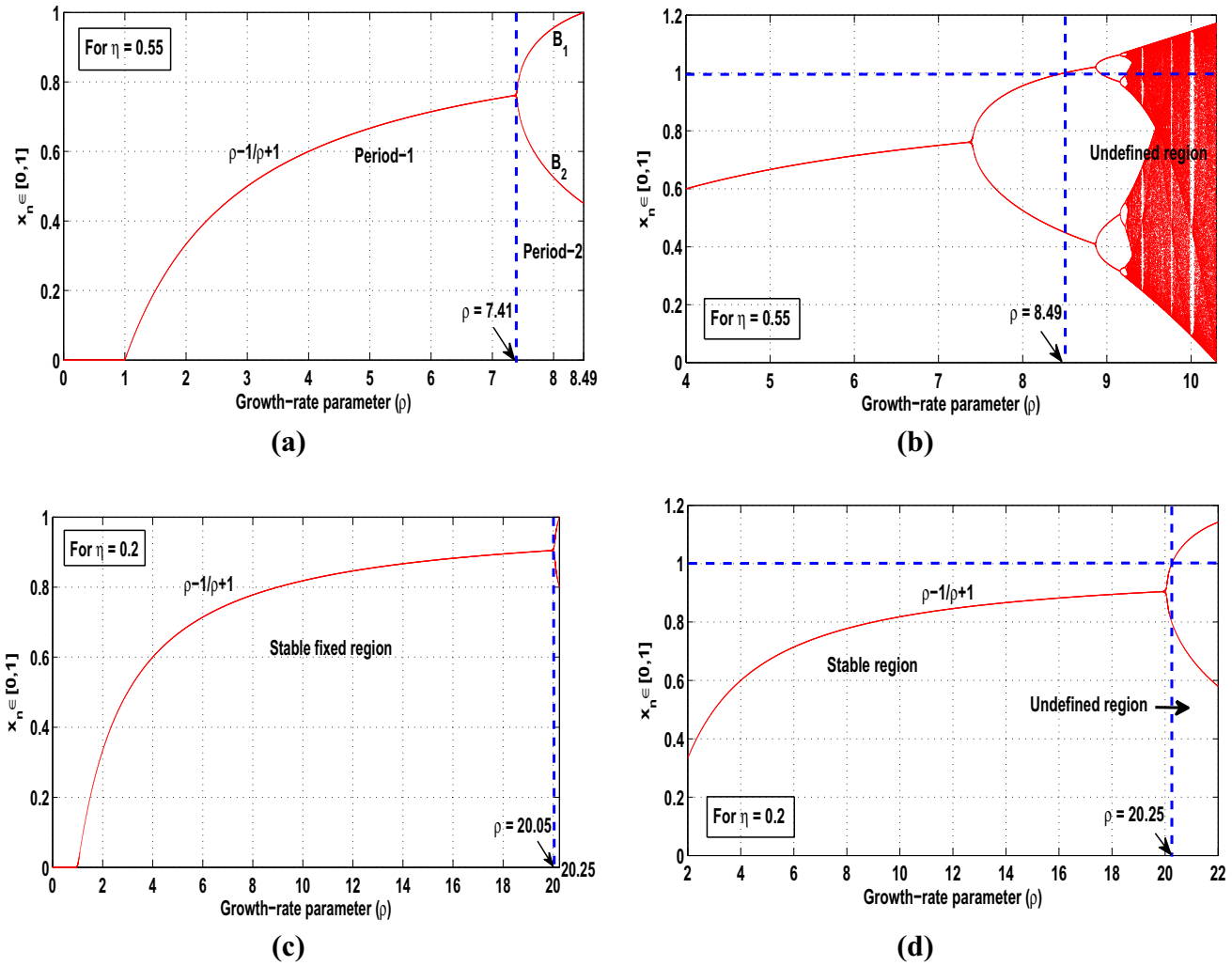

Fig. 6 For the system $T_{\eta,\rho}(x)$ with $x_0 = 0.3$ and $N = 500$, **a** period-doubling plot for $\eta = 0.55$, $0 < \rho \leq 8.49$, **b** undefined bifurcation plot for $\eta = 0.55$, $\rho > 8.49$, **c** stable region for $\eta = 0.2$, $0 < \rho \leq 20.25$, **d** undefined bifurcation plot for $\eta = 0.2$, $\rho > 20.25$

(a) the non-trivial fixed point $p_2 = \frac{\rho-1}{\rho+1}$ at $\eta = 0.9$ and $\rho = 4$,
(b) the order-two periodic points, say, $x_1 = 0.4613$ and $x_2 = 0.8114$ at $\eta = 0.9$ and $\rho = 5$.

Solution. (a) As discussed in Sect. 3.2, in the parameter extent $1 < \rho \leq 4.66$, the iteration orbit for the system $T_{\eta,\rho}(x)$ approaches to the non-trivial fixed point solution $p_2 = \frac{\rho-1}{\rho+1}$ for all $x \in [0, 1]$ and the corresponding fixed point for the iteration orbit at $\rho = 4$ is determined as $p_2 = \frac{4-1}{4+1} = \frac{3}{5} = 0.6$. So, to evaluate the maximal Lyapunov exponent (γ) for the fixed point p_2, we have to solve (17).

Since we have

$$T'_{\eta,\rho}(x) = (1-\eta) + \eta\rho\left(\frac{1-2x-x^2}{(1+x)^2}\right),$$

thus, by putting $\eta = 0.9$, $\rho = 4$ and $x = 0.6$ in above relation, we get

$$T'_{0.9,4}(0.6) = (1-0.9) + 0.9 \times 4 \times \left(\frac{1-2\times 0.6-(0.6)^2}{(1+0.6)^2}\right) = -0.6873 \tag{19}$$

Thus, from (17) and (19), we obtain

$$\gamma = \log|-0.6873| = -0.1628$$

So, the required value of MLE (γ) is -0.1628, which is less than zero. Thus, the orbit for the non-trivial fixed point $p_2 = \frac{\rho-1}{\rho+1} = 0.6$ is stable and hence it becomes a stable attractor of the system $T_{0.9,4}(x)$.

(b) Also, for $4.66 < \rho \leq 5.54$, the orbit for the system $T_{0.9,\rho}(x)$ displays order-2 periodic behavior for each $x \in [0, 1]$. At $\rho = 5$, the periodic points are calculated as, say,

$x_1 = 0.4613$ and $x_2 = 0.8114$. So,

$$T'_{0.9,5}(0.4613) = (1-0.9) + 0.9 \times 5 \times \left(\frac{1 - 2 \times 0.4613 - (0.4613)^2}{(1+0.4613)^2}\right) = -0.1853 \quad (20)$$

and

$$T'_{0.9,5}(0.8114) = (1-0.9) + 0.9 \times 5 \times \left(\frac{1 - 2 \times 0.8114 - (0.8114)^2}{(1+0.8114)^2}\right) = -1.6572 \quad (21)$$

Now, by using (18), (20) and (21), we get

$$\begin{aligned}\gamma &= \frac{1}{2}\left[\log|T'_{0.9,5}(0.4613)| + \log|T'_{0.9,5}(0.8114)|\right], \\ &= \frac{1}{2}\left[\log|-0.1853| + \log|-1.6572|\right], \\ &= \frac{1}{2}\left[-0.7321 + 0.2194\right], \\ \therefore \quad \gamma &= -0.5127\end{aligned}$$

Hence, the estimated MLE value is -0.5127, which is also less than zero. So, as a result, the periodic points of order-two, say, x_1 and x_2 are the stable attractors for the system $T_{0.9,5}(x)$.

Maximal Lyapunov exponent (γ) versus parameters η and ρ for the superior system $T_{\eta,\rho}(x)$

Now, we illustrate the maximal Lyapunov exponent (MLE) behavior of the superior discrete system $T_{\eta,\rho}(x)$ for different values of control parameter $\eta \in (0, 1)$ via showing 10,000 points for the system.

(a) For $\eta = 0.9$

The MLE plots of the system $T_{0.9,\rho}(x)$ are depicted in Fig. 7a–b. Further, Fig. 7a clearly shows that in the extent $0 < \rho \leq 5.76$, the MLE (γ) approaches to a negative value, that is, $\gamma < 0$, which signalizes the fixed stable and periodic behaviors in the system $T_{0.9,\rho}(x)$. Also, for $\rho > 5.76$, the MLE value (γ) is positive, representing chaos or irregular behavior in the system. After magnifying the MLE plot for $5.76 < \rho \leq 6.2$, an amazing behavior in the system can be reported via Fig. 7b, where the system admits extreme sensitivity to initial conditions and a fully developed chaos comes into picture.

(b) For $\eta = 0.55$

Likewise, Fig. 7c depicts that the MLE (γ) plot of the system $T_{0.55,\rho}(x)$ tends to a negative value, that means, $\gamma < 0$ for $0 < \rho \leq 8.49$. Moreover, in this range for parameter ρ, the Lyapunov spectrum exhibits two negative spikes, which characterize the fixed stable and periodic behavior of the system $T_{0.55,\rho}(x)$.

(c) For $\eta = 0.2$

The MLE ($\gamma < 0$), that means, approaches to a value less than zero in the parameter range $0 < \rho \leq 20.25$, which symbolizes stable state in the system $T_{0.2,\rho}(x)$ as displayed in Fig. 7d. Here, in the mostly extent of parameter ρ, i.e., $0 < \rho \leq 20.05$, the Lyapunov spectrum displays only one negative spike indicating the fixed stable behavior in the system $T_{0.2,\rho}(x)$.

Remark 3.5 It is evident from the above discussion that the superior system $T_{\eta,\rho}(x)$ exhibits more sensitivity to initial conditions and higher nonlinearity for large η values, as depicted for $\eta = 0.9$ in Fig. 7a and improved stability range for small η values, as shown for $\eta = 0.2$ in Fig. 7d.

4 Comparative analysis of the superior discrete chaotic system $T_{\eta,\rho}(x)$

This section deals with the comparative stability analysis of the superior discrete system $T_{\eta,\rho}(x)$ for decreasing values of control parameter $\eta \in (0, 1)$ and versus existing discrete systems in terms of comparative bifurcation and maximal Lyapunov exponent diagrams.

4.1 Comparative stability analysis w.r.t. decreasing values of control parameter $\eta \in (0, 1)$

From the comparative bifurcation plots at different values of control parameter η versus the growth-rate parameter ρ as depicted in Fig. 8, we notice that for decreasing values of the control parameter η from 1 to 0, the superior system $T_{\eta,\rho}(x)$ remains in a convergent or stable state for the higher range of the growth-rate parameter ρ. That means, the stability extent of the parameter ρ increases as we decrease the value of parameter $\eta \in (0, 1)$. Hence, it represents an inverse relation amidst the control parameter $\eta \in (0, 1)$ and the growth-rate parameter $\rho > 0$. A comparative study of the main dynamical behaviors of the superior system $T_{\eta,\rho}(x)$ versus distinct values of control parameter η is also provided in Table 1.

4.2 Comparative stability analysis of the system $T_{\eta,\rho}(x)$ versus existing discrete systems

Here, we examine the stability extent of the superior discrete system $T_{\eta,\rho}(x)$ in contrast to the canonical logistic system $f_\rho(x) = \rho x(1-x)$, logistic system in superior orbit $M_{\eta,\rho}(x)$ and the original discrete system $k_\rho(x) = \frac{\rho x(1-x)}{1+x}$. So, from the comparative Lyapunov plots shown in Fig. 9, it is reported that the red colored Lyapunov spectrum of the system $T_{\eta,\rho}(x)$ renders an enhanced stability range in contrast to the remaining Lyapunov spectrums in different colors for other systems.

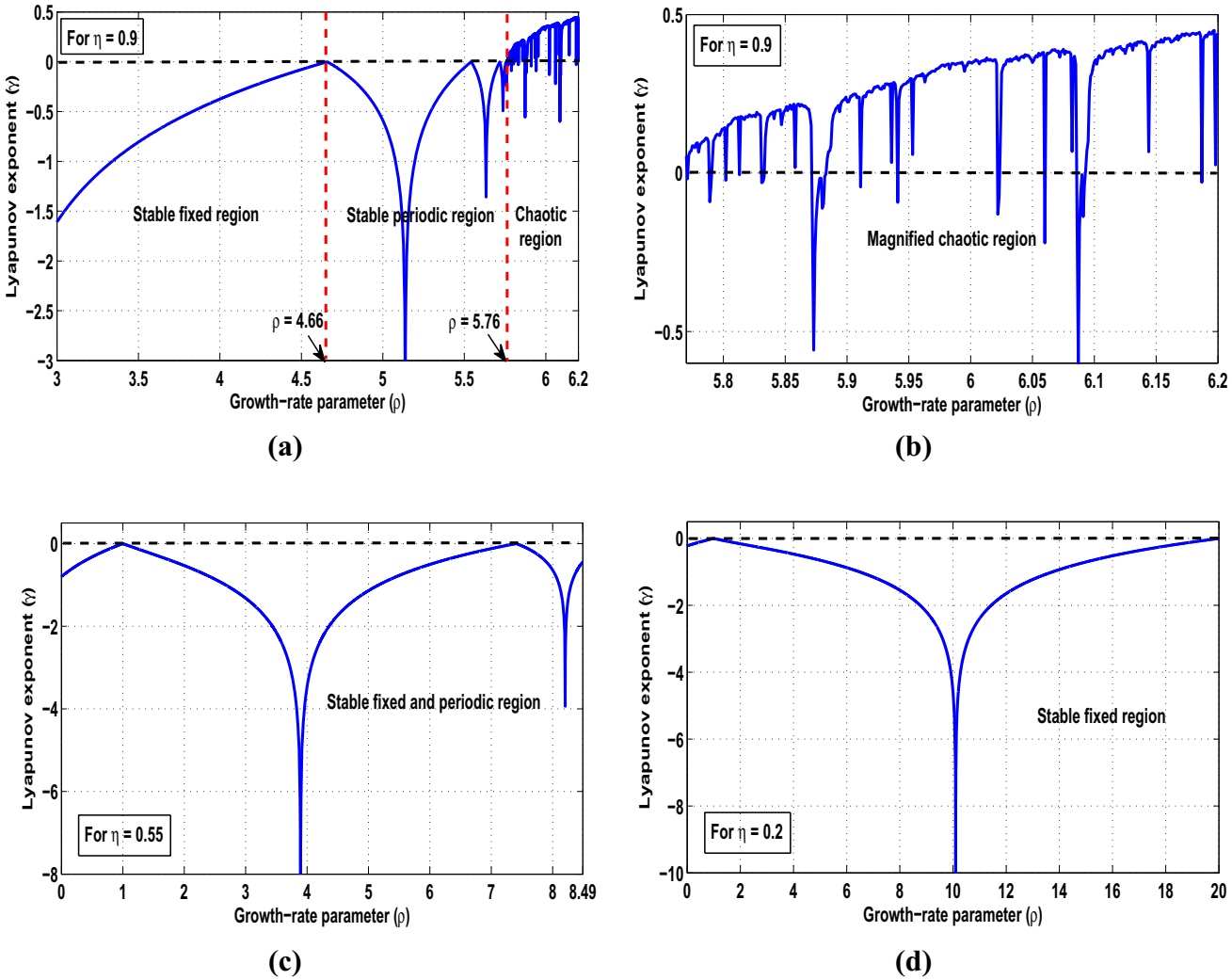

Fig. 7 For the system $T_{\eta,\rho}(x)$ with $x_0 = 0.3$ and $N = 10,000$, **a** Maximal Lyapunov exponent plot for $\eta = 0.9$, $3 \leq \rho \leq 6.2$, **b** magnified region of Lyapunov spectrum for $\eta = 0.9$, $5.77 \leq \rho \leq 6.2$, **c** MLE plot for $\eta = 0.55$, $0 < \rho \leq 8.49$, **d** MLE plot for $\eta = 0.2$, $0 < \rho \leq 20.25$

Further, Fig. 9 also depicts comparatively lower maximal Lyapunov exponent (MLE) value for the system $T_{\eta,\rho}(x)$ than that of the existing discrete systems. In addition, the lower MLE value of any system indicates the weaker sensitivity on initial conditions. Thus, the superior discrete system $T_{\eta,\rho}(x)$ having lower MLE value may be effectively used for different control-based applications.

4.3 Applications of the superior discrete system $T_{\eta,\rho}(x)$

From the above discussions, it is inferred that the superior system $T_{\eta,\rho}(x)$ displays an extensive stability range as compared to the other systems. Also, the corresponding stability range of the system further increases, when the value of control parameter η decreases from 1 to 0. Hence, owing to the enhanced stability range, the superior system $T_{\eta,\rho}(x)$ may be a better fit for different control-based nonlinear phenomena, where stability is essential like transportation problems related to traffic control (see [3, 5, 24] and other references therein).

Lo and Cho [24] proposed a discrete traffic model based on standard logistic system $f_\rho(x)$, and Ashish et al. [3] further studied that model using Mann (superior) orbit $M_{\eta,\rho}(x)$. As discussed above, the discrete chaotic system $k_\rho(x)$ admits better stability as compared to logistic system $f_\rho(x)$ and this stability range further increases under the superior system $T_{\eta,\rho}(x)$ for the decreasing values of control parameter $\eta \in (0, 1)$. Thus, motivating by applications of these discrete systems in traffic control and enhanced stability range of the superior discrete system $T_{\eta,\rho}(x)$ as compared to the existing chaotic systems, it is speculated that the proposed system might have potential applications in discrete traffic control.

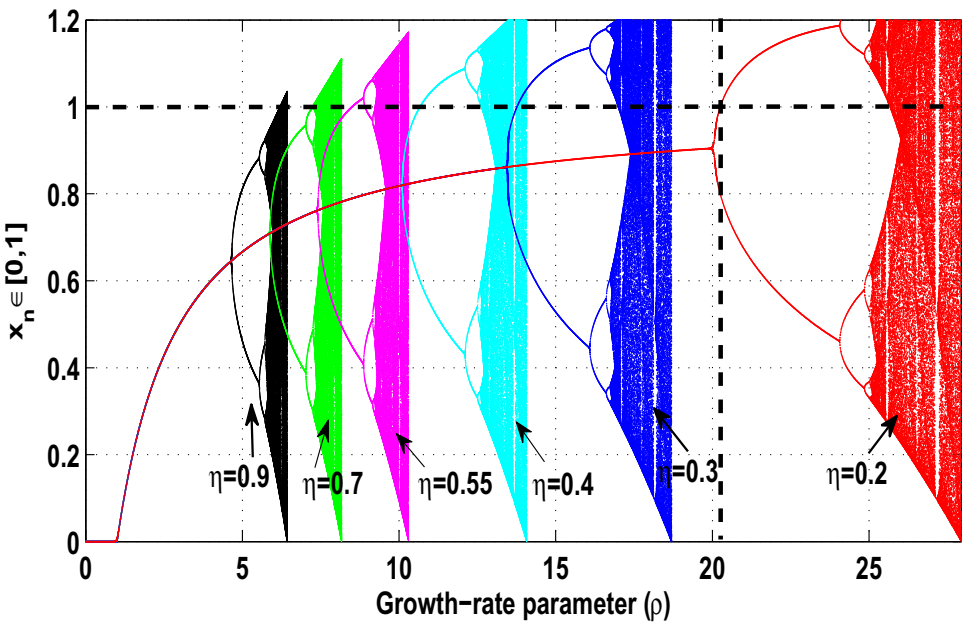

Fig. 8 Comparative bifurcation plots of $T_{\eta,\rho}(x)$ for different values of η versus parameter ρ

Table 1 Comparative dynamics table of superior system $T_{\eta,\rho}(x)$ for different η values

Dynamical behavior	$\eta = 0.9$	$\eta = 0.55$	$\eta = 0.2$
Fixed state	$0 < \rho \leq 4.66$	$0 < \rho \leq 7.41$	$0 < \rho \leq 20.05$
Periodic state	$4.66 < \rho \leq 5.76$	$7.41 < \rho \leq 8.49$	$20.05 < \rho \leq 20.25$
Chaotic state	$5.76 < \rho \leq 6.2$	–	–

So, for possible applications in traffic control, a comparative analysis of the traffic behavior via traffic control models based on different discrete systems is provided under Table 2. The different traffic states given in Table 2 mainly correspond to distinct dynamical behaviors of the discrete systems taken in Sect. 4.2 for comparative analysis via Lyapunov plots (Fig. 9). In particular, the stable (attracting) behavior of the trivial fixed point 0 corresponds to no traffic zone for different systems, whereas the stability range of the non-trivial fixed point is taken as the stable traffic state. Also, the periodic oscillations and chaos in these systems correspond to periodic stable and unstable traffic zones respectively. In superior system $T_{\eta,\rho}(x)$, the range of predictable and stable traffic state is more as compared to the other discrete systems.

5 Conclusions

This article presents a novel analysis on the stability performance of a discrete chaotic map in Mann (superior) orbit. In contrast to the original discrete map, the stable behavior in the superior system depends on two control parameters, namely η and ρ. Several dynamical aspects like fixed points, attracting and repelling fixed points, time-series representations, period-doubling bifurcations and maximal Lyapunov exponent (MLE) are interpreted thoroughly for the discrete system in superior orbit. The superior stability performance in the system with respect to decreasing values of control parameter η and versus existing discrete systems is also revealed via comparative bifurcation and MLE diagrams. The following outcomes are deduced from the analysis:

- The analysis is done for $\eta = 0.9, 0 < \rho \leq 6.2$; $\eta = 0.55$, $0 < \rho \leq 8.49$ and $\eta = 0.2, 0 < \rho \leq 20.25$, respectively, and it is revealed that the stability range of the system improves rapidly when the value of parameter $\eta \in (0, 1)$ decreases.
- At each $\eta \in (0, 1)$, the superior system admits only the trivial fixed point $p_1 = 0$ for $0 < \rho \leq 1$, which is in attracting (stable) state, whereas for $\rho > 1$, there exist two fixed points $p_1 = 0$ and $p_2 = \frac{\rho-1}{\rho+1}$ such that p_1 is repelling and p_2 is attracting for $1 < \rho \leq 4.66$ at $\eta = 0.9$, for $1 < \rho \leq 7.41$ at $\eta = 0.55$ and for $1 < \rho \leq 20.05$ at $\eta = 0.2$, respectively.
- The discrete map in superior orbit exhibits periodic behavior for the parameter extents $4.66 < \rho \leq 5.76$, $7.41 < \rho \leq 8.49$ and $20.05 < \rho \leq 20.25$ at $\eta = 0.9$, 0.55 and 0.2, respectively.
- Moreover, at $\eta = 0.9$, the irregular behavior or chaos is reported in the system for $5.76 < \rho \leq 6.2$, while for $\eta = 0.55$ and 0.2, there exists no chaos in the system.

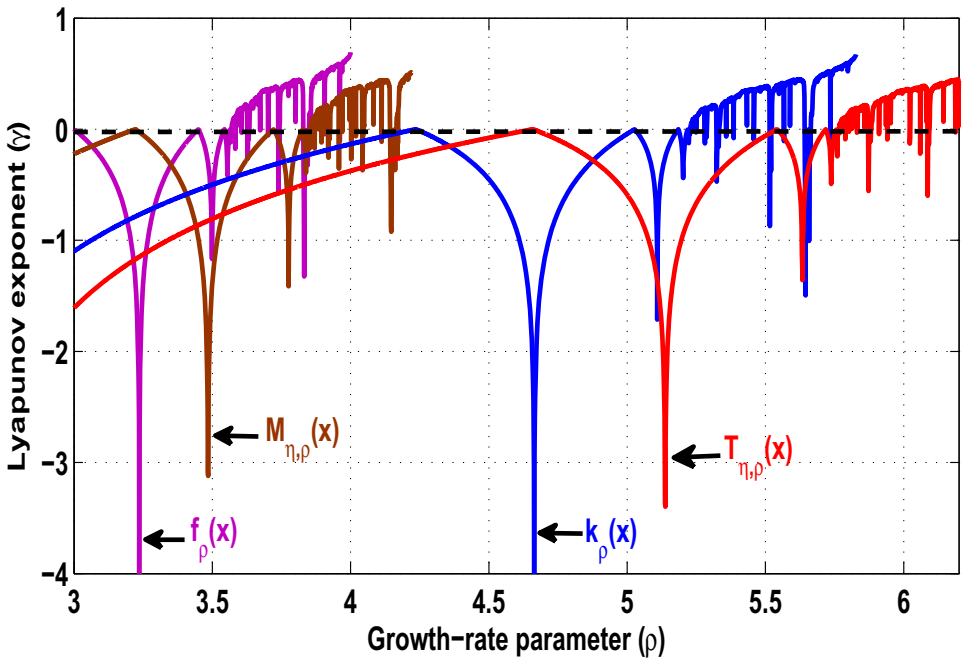

Fig. 9 Comparative Lyapunov plots of $T_{\eta,\rho}(x)$ with other discrete systems versus parameter ρ

Table 2 Comparative table of the traffic control models based on different discrete systems

Traffic behavior	$f_\rho x$	$M_{\eta,\rho}(x)$	$k_\rho x$	$T_{\eta,\rho}(x)$
No traffic on road	$0 < \rho \leq 1$	$0 < \rho \leq 1$	$0 < \rho \leq 1$	$0 < \rho \leq 1$
Stable traffic	$1 < \rho \leq 3$	$1 < \rho \leq 3.22$	$1 < \rho \leq 4.22$	$1 < \rho \leq 4.66$
$2 \leq n$-stable traffic	$3 < \rho \leq 3.57$	$3.22 < \rho \leq 3.85$	$4.22 < \rho \leq 5.21$	$4.66 < \rho \leq 5.76$
Unstable traffic	$3.57 < \rho \leq 4$	$3.85 < \rho \leq 4.22$	$5.21 < \rho \leq 5.83$	$5.76 < \rho \leq 6.2$

Thus, it is speculated that the enhanced range of stability performance of the discrete system in superior orbit in contrast to the existing discrete systems (see Sect. 4) makes it more efficient for several real-life control-based applications such as traffic control and population control in the future.

Acknowledgements The authors would like to thank the anonymous reviewers for their valuable and insightful comments that significantly helped in improving the final version of the paper. They would also like to thank the Editors for their generous comments and support.

Author Contributions All authors contributed equally to this article. They have read and approved the final manuscript.

Funding This work is supported by the University Grants Commission of India under Grant No. (F.No. 16-6(DEC. 2017)/2018(NET/CSIR) UGC Ref. No.: 1049/(CSIR-UGC NET DEC. 2017)).

Data Availability Not applicable.

Declarations

Conflict of interest The authors declare that they have no conflict of interest.

References

1. Alligood KT, Sauer TD, Yorke JA (1996) Chaos: an introduction to dynamical systems. Springer, New York
2. Andrecut M (1998) Logistic map as a random number generator. Int J Mod Phys B 12:921
3. Ashish, Cao J, Chugh R (2018) Chaotic behavior of logistic map in superior orbit and an improved chaos based traffic control model. Nonlinear Dyn 94(02):959–975
4. Ashish, Cao J (2019) A novel fixed point feedback approach studying the dynamical behaviors of standard logistic map. Int J Bifurc Chaos 29(01):1950010
5. Ashish, Cao J, Chugh R (2019) Controlling chaos using superior feedback technique with applications in discrete traffic models. Int J Fuzzy Syst 21(5):1467–1479
6. Ashish, Cao J, Chugh R (2021) Discrete Chaotification of a modulated logistic system. Int J Bifurc Chaos 31(05):2150065
7. Ashish, Cao J, Alsaadi F (2021) Chaotic evolution of difference equations in Mann orbit. J Appl Anal Comput 11(6):3063–3082
8. Ausloos M, Dirickx M (2006) The logistic map and the route to chaos: from the beginnings to modern applications. Springer, New York
9. Baptista MS (1998) Cryptography with chaos. Phys Lett A 240:50–54
10. Chowdhury AR, Debnath M (1990) Periodicity and chaos in a modulated logistic map. Int J Theor Phys 29(7):779–788
11. Chugh R, Rani M, Kumar A (2012) Logistic map in Noor orbit. Chaos Complex Lett 6(3):167–175

12. Crownover RM (1995) Introduction to fractals and chaos. Jones and Barlett Publishers, Burlington
13. Devaney RL (1948) An introduction to chaotic dynamical systems, 2nd edn. Addison-Wesley, Boston
14. Devaney RL (1992) A first course in chaotic dynamical systems: theory and experiment. Addison-Wesley, Boston
15. Diamond P (1976) Chaotic behaviour of systems of difference equations. Int J Syst Sci 7(8):953–956
16. Elagdi SN (1999) Chaos: an introduction to difference equations. Springer, New York
17. Elhadj Z, Sprott JC (2008) The effect of modulating a parameter in the logistic map. Chaos 18(2):1–7
18. de Oliveira LP, Sobottka M (2008) Cryptography with chaotic mixing. Chaos Solit Fract 35(3):466–471
19. Effah-Poku S, Obeng-Denteh W, Dontwi IK (2018) A study of chaos in dynamical systems. J Math 1808953: 5
20. Harikirishnan KP, Nandkumaran VM (1987) Bifurcation structure and Lyapunov exponent of a modulated logistic map. Pramana-J Phys 29(6):533–542
21. Holmgren RA (1994) A first course in discrete dynamical systems. Springer, New York
22. Kocarev L, Jakimoski G (2001) Logistic map as a block encryption algorthm. Phys Lett A 289:199–206
23. Kumar A, Alzabut J, Kumari S, Rani M, Chugh R (2022) Dynamical properties of a novel one dimensional chaotic map. Math Biosci Eng 19(3):2489–2505
24. Lo SC, Cho HJ (2005) Chaos and control of discrete dynamic traffic model. J Franklin Inst 342:839–851
25. Lorenz EN (1963) Deterministic nonperiodic flows. J Atmos Sci 20:130–141
26. Malek K, Gobal F (2000) Application of chaotic logistic map for the interpretation of anion-insertion in poly-orthoaminophenol films. Synth Met 11:167–171
27. Mann WR (1953) Mean value methods in iteration. Proc Am Math Soc 4:506–510
28. Martelli M (1999) Chaos: an introduction to discrete dynamical systems and chaos. Wiley-Interscience Publication, New York Inc
29. May R (1976) Simple mathematical models with very complicated dynamics. Nature 261:459–475
30. Medina RV, Mendez AD, Rio-Correa JL, Hernandez JL (2009) Design of chaotic analog noise generators with logistic map and MOS QT circuits. Chaos Solit Fract 40:1779–1793
31. Melo W, Van Strien S (1993) One-dimensional dynamics. Springer, New York
32. Mira C (1987) Chaotic dynamics. From the one-dimensional endomorphism to the two-dimensional diffeomorphism. World Scientific, Singapore
33. Mira C, Gardini L, Barugola A, Cathala J-C (1996) Chaotic dynamics in two-dimensional noninvertible maps. World Scientific, Singapore
34. Peitgen H, Jurgens H, Saupe D (2004) Chaos and fractals. Springer, New York
35. Poincare H (1899) Les methods nouvells de la mecanique leleste. Gauthier Villars, Paris
36. Radwan AG (2013) On some generalized discrete logistic maps. J Adv Res 4(2):163–171
37. Rani M, Agarwal R (2009) A new experimental approach to study the stability of logistic map. Chaos Solit Fract 41:2062–2066
38. Rani M, Goel S (2011) An experimental approach to study the logistic map in I-superior orbit. Chaos Complex Lett 5:95–102
39. Renu, Ashish, Chugh R (2022) On the dynamics of a discrete difference map in Mann orbit. Comp Appl Math 41:226
40. Renu, Ashish, Chugh R (2023) Dynamics of q-defomed logistic map via superior approach. J Appl Nonlinear Dyn 12(2):285–296
41. Robinson C (1995) Dynamical systems: stability, symbolic dynamics, and chaos. CRC Press, Boca Raton
42. Rocha JL, Taha AK (2019) Allee's effect bifurcation in generalised logistic maps. Int J Bifurcat Chaos 29(III):1950039
43. Sayed WS, Radwan AG, Fahmy HA (2015) Design of positive, negative and alternating sign generalized logistic maps. Discrete Dyn Nat Soc: 23, Article ID 586783
44. Shang P, Li X, Kamae S (2005) Chaotic analysis of traffic time series. Chaos Solit Fract 25(1):121–128
45. Sharkovsky AN, Maistrenko YL, Romanenko EY (1993) Difference equations and their applications. Kluwer Academic Publisher, Dordrecht
46. Singh N, Sinha A (2010) Chaos-based secure communication system using logistic map. Opt Lasers Eng 48:398–404
47. Strogatz SH (1994) Nonlinear dynamics and chaos. Persus Books Publishing, L.L.C., New York
48. Wackerbauer R, Witt A, Atmanspacher H, Kurths J, Scheingraber H (1994) A comparative classification of complexity measures. Chaos Solit Fract 4(I):133–173
49. Wiggins S (1990) Introduction to applied nonlinear dynamics and chaos. Springer, New York